Dissipative flux motion in high-temperature superconductors

T. T. M. Palstra, B. Batlogg, R. B. van Dover, L. F. Schneemeyer, and J. V. Waszczak
AT&T Bell Laboratories, 600 Mountain Avenue, Murray Hill, New Jersey 07974
(Received 7 July 1989)

The dissipation below T_c has been studied for representatives of all classes of cuprate high-temperature superconductors, including $Ba_2YCu_3O_{7-\delta}$, and Bi and Tl compounds. The results are parametrized in the framework of flux creep, with the largest activation energies found in $Ba_2YCu_3O_7$. It is argued that the magnitude of dissipative flux motion is more related to the electronic anisotropy of the material than the actual defect structure. The thermally activated flux creep model, whose parameters are extracted from dc measurements, consistently describes also dynamic measurements, including the irreversibility line and the melting transition. Finally, the similarities in dissipative behavior are emphasized between high-T_c materials, very thin films, and layered low-T_c superconductors.

I. INTRODUCTION

Vortex dynamics in superconductors reveals information about the motion of vortices as influenced by various interactions and is related to an important technological quantity: the depinning critical current. This research area has recently been very fruitful, and is studied using various experimental techniques, such as time dependence of the remanent magnetization,[1-3] dc resistivity,[4-9] ac susceptibility,[10,11] microwave absorption, the mechanical oscillator[12,13] and decoration experiments.[14,15] The aim of this paper is to provide a consistent phenomenological model for the various experiments. In particular we will focus on five issues: (1) the value of the depinning critical current in a magnetic field, (2) the difference in pinning for the various high-temperature superconductors, (3) the actual value of the activation energy for flux motion, (4) the relation between static and dynamic experiments, and (5) the comparison between high-T_c and low-T_c materials.

Starting with a discussion of the dc-resistivity results, we will parametrize these measurements in terms of a flux creep model, from which we can estimate several microscopic parameters, in particular the activation energy of vortex dynamics. These activation energies are compared for the various high-temperature superconductors, and related to the tilt modulus of the flux lines, which is in part determined by the electronic coupling between the Cu-O double planes. It turns out that this coupling strength between the Cu-O planes determines the pinning behavior more than the actual defect structure. Furthermore, we will use thermally activated vortex dynamics to relate our dc measurements with ac experiments. This model gives the intimate relationship between the dc resistivity and ac susceptibility, and furthermore makes the connection between the melting line and the irreversibility line. Finally, we compare our resistivity measurements on the high-T_c materials with measurements on low-T_c materials, in which similar behavior has been observed.

II. EXPERIMENTAL TECHNIQUES

The crystal growth of the various compounds and a detailed characterization of the crystals has been described elsewhere.[16-18] Typically, we used single crystal samples of $1\times0.2\times0.01$ mm^3 with four sputtered Ag contacts. After sputtering, Ag leads were attached using Ag epoxy, and annealed for 2 hours at 250 °C. The contact resistance is generally as small as the sample resistance at room temperature, and does not contribute significantly to heating. The current-voltage (I-V) characteristics were carefully measured, and the temperatures at which linear I-V behavior was observed are marked in Figs. 2 and 8. The temperature was measured with a calibrated carbon-glass thermometer and accurate corrections for its magnetoresistance were made. A magnetic field up to 12 T was generated by a superconducting solenoid.

III. EXPERIMENTAL RESULTS AND DISCUSSION

A. $Bi_2Sr_2CaCu_2O_8$

In Fig. 1 we show the resistive transition of $Bi_2Sr_2CaCu_2O_8$ in magnetic fields of 0, 2, 5, and 12 T both perpendicular and parallel to the a,b basal planes. The inset shows the zero-field transition up to 300 K. The transition in zero field is very sharp, but broadens considerably upon applying a field. The upper part of the figure shows the full range of the resistivity up to the normal state. We focus in this paper upon the low-resistivity data, which are shown on an expanded scale in the lower part of the figure. As we discuss later we cannot use a resistivity criterion to determine H_{c2}.

In order to show the low-resistance data more clearly, we replot the resistivity data in Fig. 2 on a logarithmic scale, versus inverse temperature for four magnetic fields 0, 0.1, 1, and 10 T perpendicular to the a,b basal plane. While the anomaly at T_c is very small in this presentation of the data, this Arrhenius plot shows that the resistivity is thermally activated over four orders of magnitude from 10^{-4} to 1 $\mu\Omega$ cm below about 1 $\mu\Omega$ cm or 1% of the

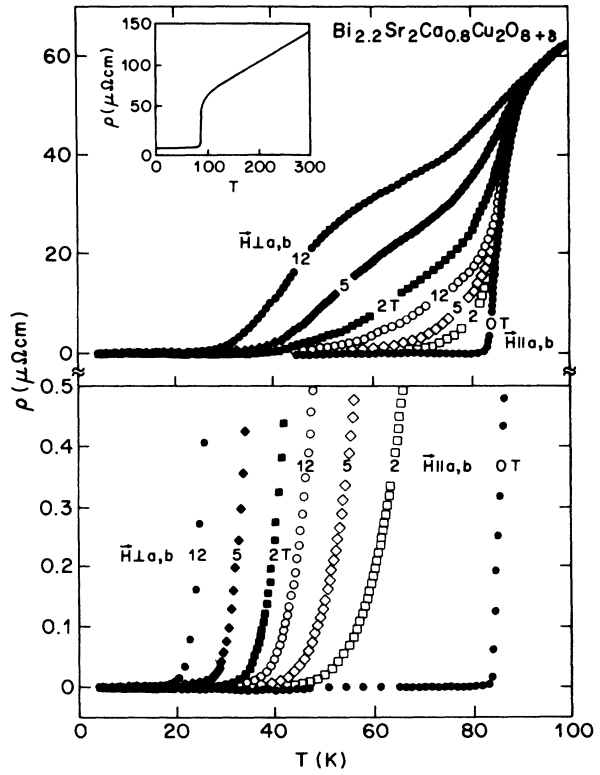

FIG. 1. Temperature dependence of the electrical resistivity $Bi_2Sr_2CaCu_2O_8$ in four selected magnetic fields, 0, 2, 5, and 12 T, oriented parallel (open symbols) and perpendicular to the basal planes. The lower part of the figure is a magnification by about a factor 100 to emphasize the exponential behavior. The inset shows the zero-field resistivity up to room temperature.

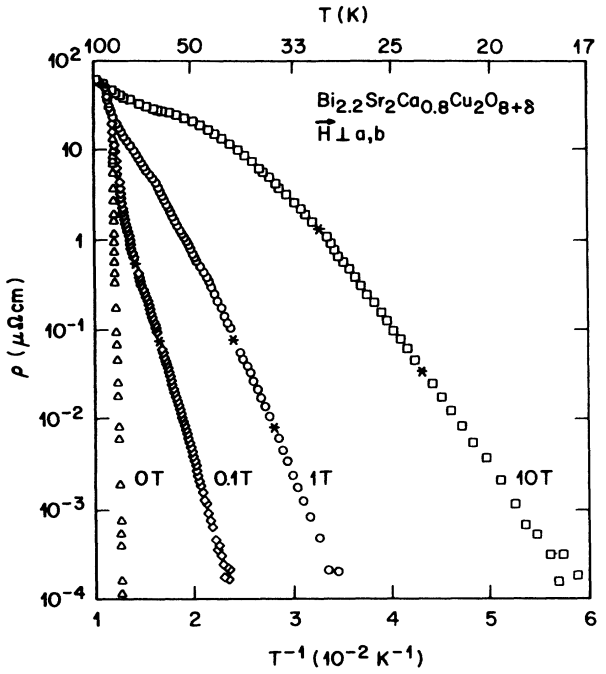

FIG. 2. Arrhenius plot of the resistivity of $Bi_2Sr_2CaCu_2O_8$ in four selected magnetic fields, 0, 0.1, 1.0, and 10 T, perpendicular to the basal planes. The asterisks denote the temperatures at which ohmic dissipation (linear I-V) was measured (see Fig. 7).

normal-state resistivity, from 17 to 75 K, and from 0.1 to 12 T. The slope of the curves below this 1% criterion is related to the activation energy U_0 (a more detailed discussion on this point is given in a subsequent section), and the resistivity can therefore be described as

$$\rho(T,H,\phi)=\rho_0\exp(-U_0/k_BT) . \quad (1)$$

The temperature scale for the activation energy can be normalized as U_0/T. This is shown in Fig. 3 for three magnetic fields 0.1, 1, and 10 T perpendicular to the basal plane. All curves coalesce on one line which means that the preexponential factor ρ_0 is field independent. The value of ρ_0 is about 10^5 $\mu\Omega$ cm, about three orders of magnitude larger than the normal-state resistivity.

For the other orientation **H∥a,b** we also find thermally activated behavior well below T_c, however with different activation energies. The values for U_0 range from 300 to 3000 K. Using the normalized temperature scale U_0/T, the curves for this orientation coalesce with the **H⊥a,b** data. Therefore, the preexponential factor ρ_0 is not only field independent, but also orientation independent.

Finally, in Fig. 4 we show the magnetic field dependence of the activation energy U_0. This plot suggests a power law dependence $U\sim H^{-\alpha}$ with $\alpha\simeq\frac{1}{2}$ for $H_\perp<3$ T, $\alpha\simeq\frac{1}{3}$ for $H_\perp>3$ T, and $\alpha\simeq\frac{1}{3}$ for $H_\parallel<3$ T, and $\alpha\simeq\frac{1}{4}$ for $H_\parallel>3$ T. More significantly, we find that U_0 does not scale with H^{-1}.

We note here that the values of U_0 for different fields H are deduced from different limited temperature ranges.

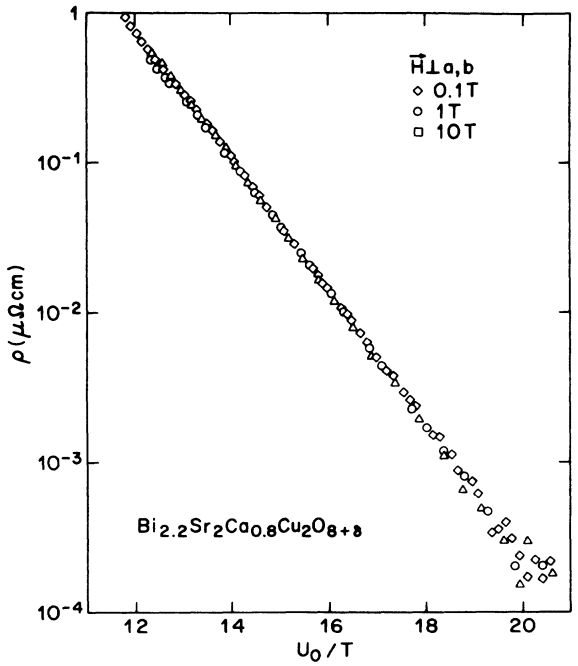

FIG. 3. Universal behavior of the thermally activated electrical resistivity for the data of Fig. 2, by use of a normalized temperature scale U_0/T.

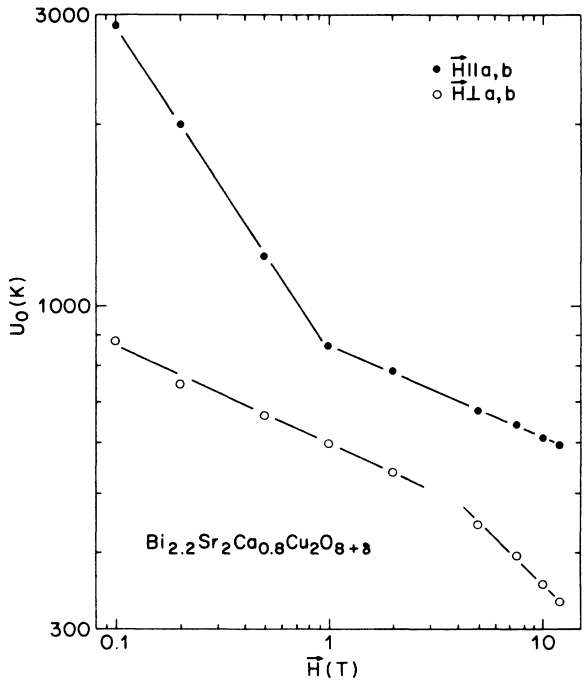

FIG. 4. Magnetic field dependence of the activation energy U_0 for flux creep in two orientations, determined from the Arrhenius curve between 10^{-4} and 1 $\mu\Omega$ cm.

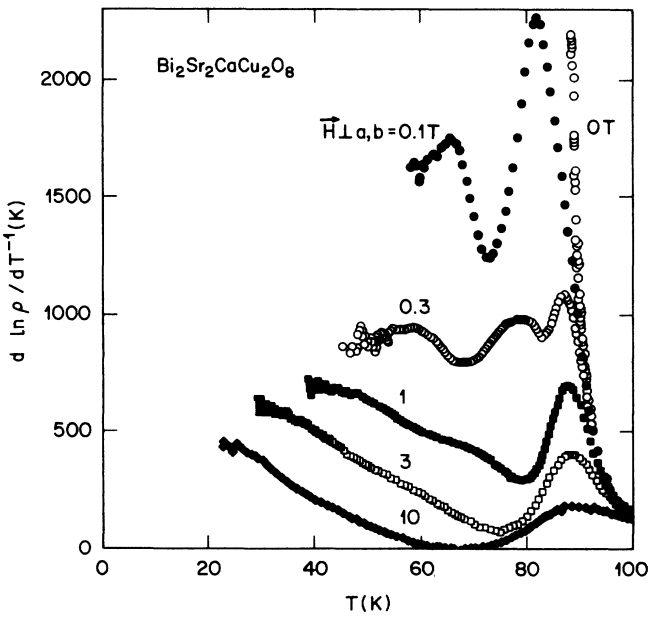

FIG. 5. Temperature dependence of $d\ln\rho/dT^{-1}$ (i.e., the slope of the Arrhenius curve). This sample has a slightly higher activation energy than the sample of Figs. 2 and 4. The activation energy in Fig. 4 was determined in the temperature interval over which the resistivity changes from 10^{-4} to 1 $\mu\Omega$ cm. Flux creep applies only for $T \ll T_c$, $U_0 > k_B T$, and $\rho \ll \rho_n$.

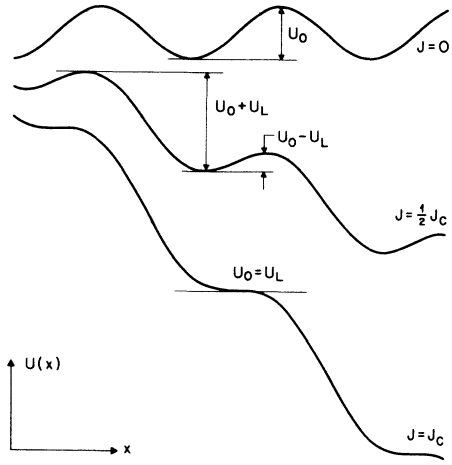

FIG. 6. Schematic representation of the condensation energy along the coordinate of the Lorentz force. The upper curve shows the unperturbed potential U_0, and the lower curve shows depinning ($U_0 = U_L$).

The values of U_0 are determined from the limited temperature interval over which the data on the Arrhenius plot can be represented by a straight line. Even if the slope does not change significantly in the temperature interval in which the resistivity changes by four orders of magnitude, it does not mean that U_0 is temperature independent. A temperature dependence of U_0 can be probed by plotting the temperature dependence of $d\ln\rho/dT^{-1}$ (i.e., the slope of the Arrhenius curve), as shown in Fig. 5. Obviously, the values of U_0 shown in Fig. 4 are determined in a narrow temperature interval, in which U_0 is fairly constant but in which ρ still changes by four orders of magnitude.

It is not clear from Fig. 5 whether U_0 is constant below this temperature interval. At higher temperatures, a flux creep description is only applicable if $U_0 > k_B T$. If the barriers become comparable to thermal energies, a diffusion model, corresponding to flux flow, is more appropriate than a hopping model for flux creep. Near T_c different processes dominate,[19,20] which give rise to the sharp peak near 85 K in Fig. 5. [Note: Interpretation of the slopes in terms of activation energies is meaningless in this range of $\rho(T)$ curves.]

We will discuss and parametrize this thermally activated dissipation in terms of a flux creep model, as proposed by Anderson and Kim.[21,22] This assumes that flux lines are well defined objects. In any superconductor in the mixed state the flux lines will be pinned due to various interactions, e.g., impurities, stress, extended defects, etc. The basic concept of flux creep is that a flux line or flux bundle can be thermally activated over the pinning energy barrier, even if the Lorentz force exerted on the flux bundle by the current is smaller than the pinning force (Fig. 6). The rate with which this process occurs is given by the attempt frequency, the value of the unperturbed pinning potential U_0, and the Lorentz force energy U_L.

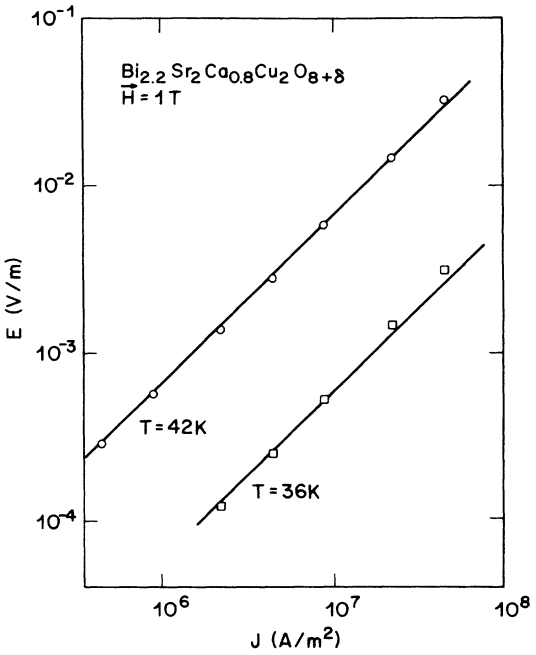

FIG. 7. Double logarithmic plot of the electric field vs current density (or I-V curve) to emphasize the large range over which the dissipation is ohmic. The slope of the curves is 1.

The rate of forward hopping (in the direction of the Lorentz force) is then given by

$$\nu_0 \exp[-(U_0 - U_L)/k_B T]$$

and the rate of reverse hopping (opposite the direction of the Lorentz force) is given by

$$\nu_0 \exp[-(U_0 + U_L)/k_B T] .$$

This results in a net hopping rate:

$$\nu_{\text{eff}} = \nu_0 \exp(-U_0/k_B T) \sinh(U_L/k_B T) . \quad (2)$$

The Lorentz force energy U_L is given by the Lorentz force density $F_L = \mathbf{J} \times \mathbf{B}$, the volume of the flux bundle V_c that moves independently of the other flux bundles, and the range of the pinning potential r_p:

$$U_L = (\mathbf{J} \times \mathbf{B}) V_c r_p . \quad (3)$$

In addition to thermal activation, this model predicts a linear I-V curve for small current densities, which can be checked experimentally. For current density J for which $U_L \lesssim k_B T$, $\sinh(x) \simeq x$ and the average flux velocity $v_\phi = \nu_{\text{eff}} L$, with L the hopping distance, is proportional to the current density:

$$v_\phi = 2\nu_0 L \frac{JBV_c r_p}{k_B T} \exp(-U_0/k_B T) . \quad (4)$$

The linearity of $v_\phi(J)$ or $E(J)$ with the electric field E is confirmed in Fig. 7 in a double logarithmic plot. The lines through the data points have slope 1.

The range over which ohmic dissipation is observed ($E \propto J$) sets an upper limit on the flux bundle volume V_c. E is proportional to J only if $JBV_c r_p \lesssim k_B T$. Assuming that the pinning in this material is governed by point defects, or that $r_p \approx \xi_{GL}$, the Ginzburg-Landau coherence length, we find that at least for high fields the flux bundle volume V_c cannot be much larger than $a_0^2 d$, which is the volume of one flux line (a_0 is the flux line separation and d the sample thickness). It is possible that the bundle volume is even smaller than this value, if the length of the bundle (the correlation length L_c) is shorter than the sample thickness d. This means that at least for large magnetic fields and the temperature range probed here the flux line lattice is in the "amorphous limit," or $V_c \approx a_0^2 L_c$. Assuming that the hopping distance is of the order of a_0, we can rewrite Eq. (4) as

$$\rho = \frac{v_\phi B}{J} = \frac{2\nu_0 \phi_0^2 L_c}{k_B T} \exp(-U_0/k_B T) . \quad (5)$$

Comparing this result with our experimental result of Eq. (1), one can relate the preexponential factor ρ_0 to the attempt frequency ν_0. Assuming that $L_c \approx 0.1d$, we find that $\nu_0 \approx 10^{12}$ Hz.

For large current densities but still in the flux creep regime $J \gtrsim k_B T/BV_c r_p$ this linear $E(J)$ behavior will turn into an exponential behavior [see Eq. (2)]. This is the re-

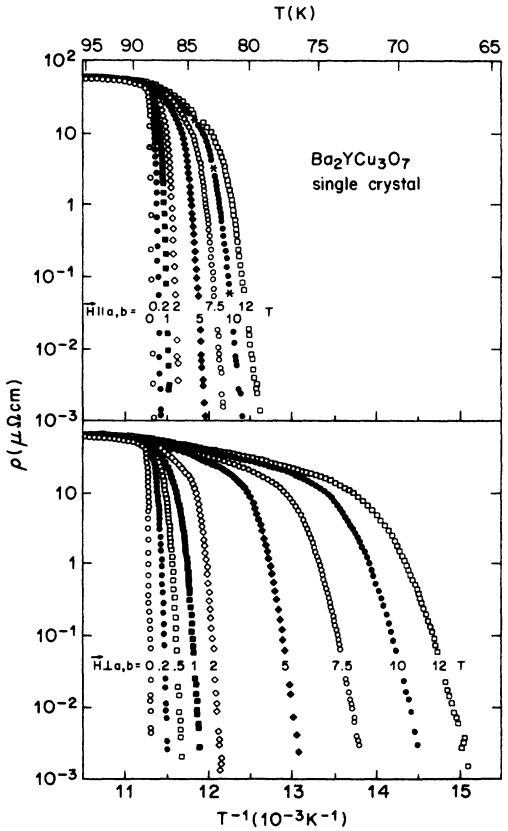

FIG. 8. Arrhenius plot of the resistivity of $Ba_2YCu_3O_7$ for magnetic fields parallel to the basal plane (upper panel), and perpendicular to the basal plane (lower panel). The asterisks denote the temperatures at which ohmic dissipation (linear I-V) was measured (see Fig. 11).

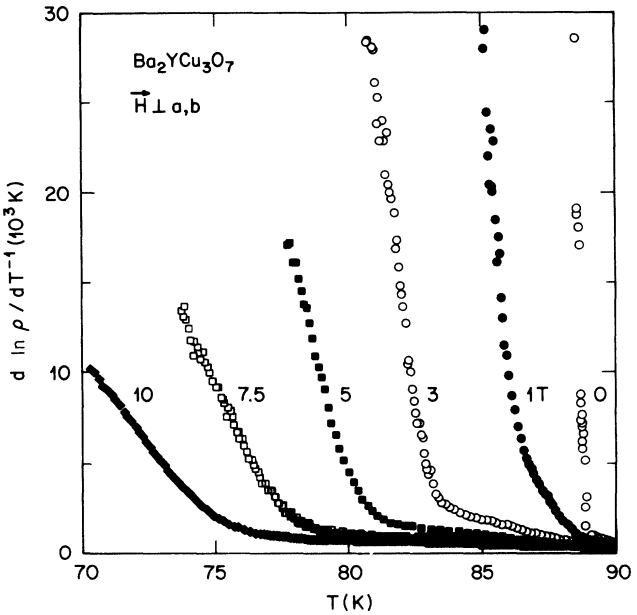

FIG. 9. Temperature dependence of $d\ln\rho/dT^{-1}$ for single crystal $Ba_2YCu_3O_7$ (i.e., the slope of the Arrhenius curve). This value is not the activation energy for flux creep $U_0(t)$ at this temperature, but enhanced by a factor $[1+qt/(1-t)]$ (see Fig. 10).

gime in which flux creep has been studied in traditional superconductors. In these materials the current densities to obtain linear E-J characteristics are much smaller than in the high-T_c materials, because (1) thermal energies are much smaller, (2) V_c is larger, and (3) r_p is larger because the coherence lengths are larger for low-temperature superconductors.

Depinning occurs when $U_0 = U_L$ which means that the effective barrier height $U_0 - U_L$ has been reduced to zero (see Fig. 6). For these currents one gets in the regime of flux flow, where the flux line velocity is no longer determined by the probability of hopping over an energy barrier, but by the viscosity (or the mutual interactions) within the vortex system. For low-temperature superconductors this regime was successfully described by the Bardeen-Stephen model[23] which gives for the flux flow resistance $\rho_f = \rho_n H/H_{c2}$ with ρ_n the normal-state resistivity. For the high-temperature superconductors the applicability of this model has not yet been explored.

B. $Ba_2YCu_3O_7$

In this section we will discuss the resistivity of $Ba_2YCu_3O_7$ in the framework of Anderson-Kim flux creep. In Fig. 8 we show the Arrhenius plot of the resistive transition of $Ba_2YCu_3O_7$. As for the Bi compound, the thermally activated part of the resistance transition sets in below approximately 1% of the normal-state resistivity. However, the resistivity drops more rapidly than in the Bi compound, and thus the temperature range of the measurements is much smaller. The slope of these Arrhenius plots for low resistivity can be related to the activation energy for flux creep. The values of the slopes range from 10^4 K to 2×10^5 K for magnetic fields between 0.1 and 12 T.

Thus far, we have analyzed only the lowest-temperature part of the $R(T)$ curve, characterizing it by U_0. A temperature dependence of the activation energies can be shown by plotting the slope of the Arrhenius curve $d\ln\rho/dT^{-1}$ versus T (Fig. 9). In contrast to the visual observation of Fig. 8, this mathematical treatment reveals how rapidly the slopes change with temperature, without attaining a constant value.

C. Temperature dependence of the activation energy

It should be emphasized that the Arrhenius curve slopes are directly related to, but not equal to, the activation energies. Namely, using a typical slope of 10^4 K at 70 K and 10 T (as shown in Fig. 9) as activation energy, gives a resistivity $\rho = \rho_0 \exp(-10^4/70) \approx 10^{-58}$ $\mu\Omega$ cm, assuming a ρ_0 of similar order of magnitude as found for the Bi compound. Clearly, the true activation energy at 70 K and 10 T must be much smaller in order to obtain a measurable resistivity of $\rho(70\text{ K}, 10\text{ T}) \simeq 10^{-2}$ $\mu\Omega$ cm.

In a proper analysis of temperature dependence of the resistivity, the temperature dependence of the superconducting parameters has to be taken into account *explicitly*. For demonstration, we consider a simple case, with only a temperature dependent activation energy (neglecting the temperature dependence of the prefactor). A conventional choice[24] is $U_0(t) \propto H_c^2(t)\xi^n(t)$, with n between 0 and 3. Using the parabolic approximation $H_c(t) \propto 1-t^2$ and $\xi^2(t) \propto (1+t^2)/(1-t^2)$, we find

$$U_0(t) = U_0(0)\frac{(1-t^2)^q}{(1+t^2)^{q-2}}\ , \tag{6}$$

with $q = 2 - n/2$. This function is shown in the upper panel of Fig. 10 for $q = 1$, as suggested in Ref. 24, and $q = 1.5$, as proposed by Refs. 2 and 5. Near T_c this function can be approximated by

$$U_0(t) = U_0(0)(1-t)^q\ , \tag{7}$$

with $t = T/T_c$. Combining Eq. (7) with a thermally activated resistivity [Eq. (1)], we find that the slope of the Arrhenius curve near T_c is given by

$$\frac{d\ln\rho}{dT^{-1}} = U_0(0)(1-t)^q[1+qt/(1-t)]\ . \tag{8}$$

Thus, near T_c the apparent activation energy derived from the Arrhenius curve slope is enhanced with respect to the actual value by $[1+qt/(1-t)]$. The enhancement is significant near T_c, where U_0 is strongly temperature dependent, but is negligible for $t < 0.5$ where U_0 is almost constant. The lower panel of Fig. 10 shows the slope of the Arrhenius curve over the entire temperature regime up to T_c for the activation energy given by Eq. (6) for $q = 1$ and 1.5. This temperature dependence of the activation energy gives a consistent description for the values of the activation energies and the preexponential factor ρ_0. To show this, we consider one particular example.

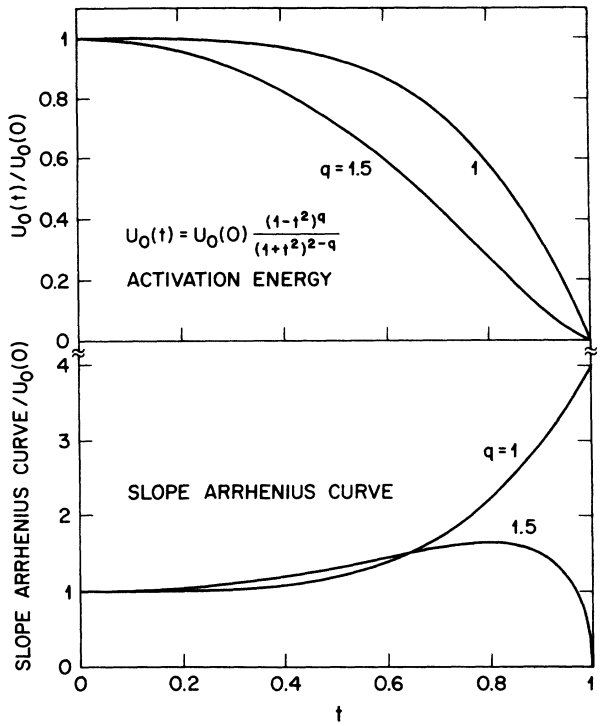

FIG. 10. Temperature dependence in reduced units of an assumed activation energy $U_0(t)$ for two values of q, and the corresponding slopes of an Arrhenius plot, which are enhanced near T_c by a factor $[1+qt(1-t)]$. The difference is pronounced near T_c.

Assuming $q=1.5$, we find that at $H=10$ T and $T=70$ K or $t=0.93$ that the enhancement factor $1+qt/(1-t)=20$, and thus the activation energy $U_0\simeq 10^4/20=500$ K (see Figs. 9 and 10). This results in a value for the preexponential factor $\rho_0=\rho\exp(U_0/k_BT)\simeq 10\ \mu\Omega$ cm. For $q=1$ we obtain $U_0(0.93)\simeq 715$ K and thus $\rho_0\simeq 3\times 10^2\ \mu\Omega$ cm. These values are thus in the similar range as observed for the Bi compound. However, activation energies of the order of 500 K were observed for the Bi compound at low temperatures $t<0.5$, whereas for $Ba_2YCu_3O_7$ these values are already obtained in the vicinity of T_c ($t>0.93$). This strongly suggests that the zero-temperature activation energies are much larger for $Ba_2YCu_3O_7$ than for the Bi compounds.

Our data are consistent with the specific temperature dependence which was suggested[2] to explain the magnetic relaxation data: $U_0\propto(1-t)^{3/2}/B$. However, because of the limited temperature regime accessible for the measurements of $Ba_2YCu_3O_7$ we cannot rule out other temperature and field dependences of the activation energy, e.g., the "glassy model,"[25] or the thermally assisted flux flow model.[11]

Besides the correct temperature dependence of $U_0(T)$, also the appropriate magnetic field dependence of the transition temperature $T_c(H)$ has to be taken into account.[26] Thus far many analyses[3,7,8] assumed a magnetic field independent transition temperature, derived from the zero-field data, which we argue is incorrect. Figure 9 shows that the activation energies extrapolate linearly to zero at a temperature T_x, much below the zero-field transition temperature. We find for example that $T_x\approx 75.5$ K for $H_\perp=10$ T, and $T_x\approx 81$ K for $H_\perp=5$ T. We think that any scaling should use this temperature $T_x(H)$ instead of $T_c(H=0)$. This temperature denotes the transition, where the activation energies become comparable to thermal energies. Therefore, below T_x we are in the regime of flux creep, and above T_x the dissipation is dominated by flux flow and fluctuations.

In conclusion, we have shown that the temperature dependence of the resistivity below $10^{-2}\rho_n$ can be described with a thermally activated model. For the Bi compound an analysis neglecting the temperature dependence of U_0 gives activation energies from 300 to 3000 K for magnetic fields between 0.1 and 12 T, and a preexponential factor $\rho_0\simeq 10^5\ \mu\Omega$ cm. From our data it is not clear whether a temperature independent activation energy is appropriate, even though the measurements were performed down to low temperatures ($t<0.5$). Taking a temperature dependence of U_0 into account will decrease the value of the preexponential factor ρ_0 down to values expected from the Bardeen-Stephen model $\rho_0\sim\rho_nH/H_{c2}$. However, for $Ba_2YCu_3O_7$ the activation energies increase more rapidly below T_c, which restricts resistivity measurements to a temperature regime $t>0.93$. In this regime the temperature dependence of the activation energy has to be taken explicitly into account. The preexponential factor ρ_0 is of the same order of magnitude as for the Bi compound, but its exact value depends on the appropriate temperature dependence of U_0, which we argue remains ambiguous.

D. *I-V* curves

The resistivities shown in Figs. 8 are also taken in the ohmic dissipation regime (linear current voltage). This is shown in the inset of Fig. 11, which shows the electric field versus current density in a double logarithmic scale. The lines through the data points have slope 1. At current densities larger than 10^6 A/m^2 deviations occur from linearity, reflecting either the transition into the exponential part of the flux creep regime and/or heating effects. Because of the large dissipation in the high-current regime, we were unable to take data here but have sketched the current-voltage dependence in the main part of the figure. In the presence of a magnetic field, only at zero temperature can a sharp transition from zero resistance to finite resistance be observed at the depinning critical current. At finite temperature there is a finite slope in the *I-V* curve due to flux creep.

An *I-V* curve can intercept a 1-μV criterion, which is commonly used to define the depinning critical current I_c, at a current density much lower than the actual depinning current. This is illustrated by taking in the inset of Fig. 11 criterion of 1 μV/mm as voltage criterion. Clearly, the current densities corresponding with the 1-μV/mm criterion are not the depinning current densities because the *I-V* curve is still linear. Depinning takes place at larger current densities above the linear regime

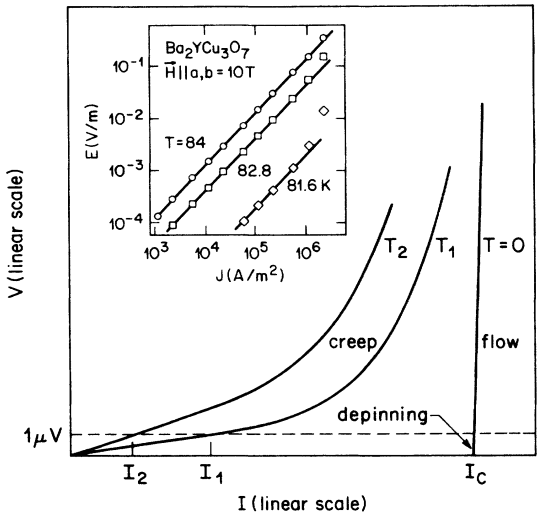

FIG. 11. Schematic representation of I-V curves for the high-temperature superconductors. At $T=0$ the true depinning critical current is observed, but at higher temperatures flux creep results in dissipation and a 1-μV criterion gives an arbitrary current density. The inset shows three experimental I-V curves for $Ba_2YCu_3O_7$ on a double logarithmic scale to emphasize the large ohmic dissipation regime. The slope of the curves is 1.

of I-V and can only be measured properly at $T=0$. Therefore, the depinning critical currents in a magnetic field can be much larger than indicated by a 1-μV criterion. However, this current does not indicate the value below which no dissipation occurs, as for the technical superconductors, in which flux creep is insignificantly small. We conclude that any voltage criterion to define the depinning critical current is arbitrary and meaningless for the high-temperature superconductors in the presence of a large magnetic field. A practical consequence is that this apparently precludes the use of the Bi compound in large fields above 4.2 K, and $Ba_2YCu_3O_7$ in fields above several Tesla above 77 K.

In the case of these materials it is more appropriate to use the resistivity in the low-current limit ($U_L < U_0$). In order to compare $Bi_2Sr_2CaCu_2O_8$ and $Ba_2YCu_3O_7$ we show in Fig. 12 the temperature dependence of the resistivity (on a logarithmic scale) of both materials in magnetic fields of 0, 1, and 12 T. As a reference the resistivity of Cu is also shown. The resistivity of $Bi_2Sr_2CaCu_2O_8$ in large magnetic fields only dips below the value of copper under $\sim$4 K. Even for $Ba_2YCu_3O_7$ the resistivity at 77 K in large magnetic fields is larger than the value of copper and is only smaller than copper at 77 K for magnetic fields below a few Tesla.

E. Pinning

In this section we want to discuss the difference in pinning behavior between $Bi_2Sr_2CaCu_2O_8$ and $Ba_2YCu_3O_7$. It has been argued that the large activation energies in the latter compound stem from the presence of twin planes, which form extended defects. In contrast, the dominant pins in $Bi_2Sr_2CaCu_2O_8$ are speculated to be point defects, due to extensive cross substituting resulting in much smaller activation energies. We think that this difference in defect structure is *not* the origin of the difference in pinning energies.

We argue that the different pinning energies stem from the difference in anisotropy. Namely, it has been shown that the anisotropy in electronic properties is much larger in $Bi_2Sr_2CaCu_2O_8$ than in $Ba_2YCu_3O_7$.[27,28] A large electronic anisotropy directly results in a reduction of the tilt modulus of the flux lines, which means that the correlation length along the flux lines L_c is reduced. In the extreme limit of completely decoupled layers, there is no correlation between the vortices in adjacent planes, and L_c is reduced to the interlayer spacing. A short correlation length along the vortices L_c results in small activation energies, because of the small flux bundle volume:

$$U_0=\mathbf{J}_c\times\mathbf{B}V_c r_p=\mathbf{J}_c\times\mathbf{B}R_c^2L_c r_p\ , \tag{9}$$

with R_c the correlation length of the vortices in the planes, and L_c the correlation length along the vortex. Assuming we are in the amorphous limit of the vortex system ($R_c=a_0$), and that the main defects are point defects ($r_p\approx\xi_{GL}$), this relation reduces to

$$U_0=\mathbf{J}_c\times\boldsymbol{\phi}_0 L_c\xi_{GL}\ . \tag{10}$$

Large flux creep is thus favored by (1) small values of L_c which is intrinsic to large anisotropy compounds and thin films and (2) a short coherence length which holds for extreme type-II superconductors including the high-T_c superconductors.

This interpretation is corroborated by two experimental findings: (1) The layered compound $NbSe_2$ with a low transition temperature $T_c=7.2$ K and various other thin film superconductors have as large flux creep effects[29] as the high-temperature superconductor $Bi_2Sr_2CaCu_2O_8$,

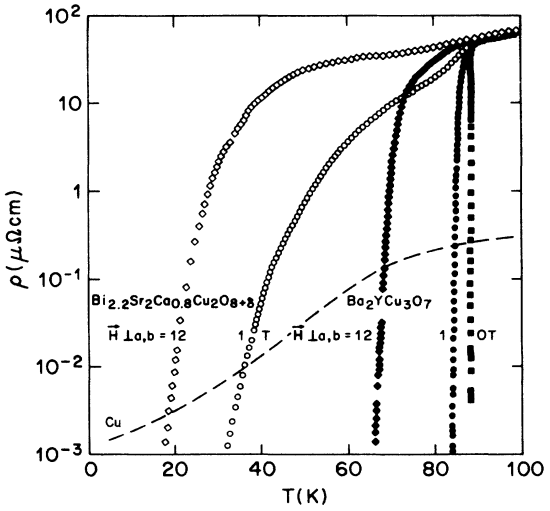

FIG. 12. Temperature dependence of the electrical resistivity $Bi_2Sr_2CaCu_2O_8$ and $Ba_2YCu_3O_7$ on a semilogarithmic scale. The curve of copper is given for reference.

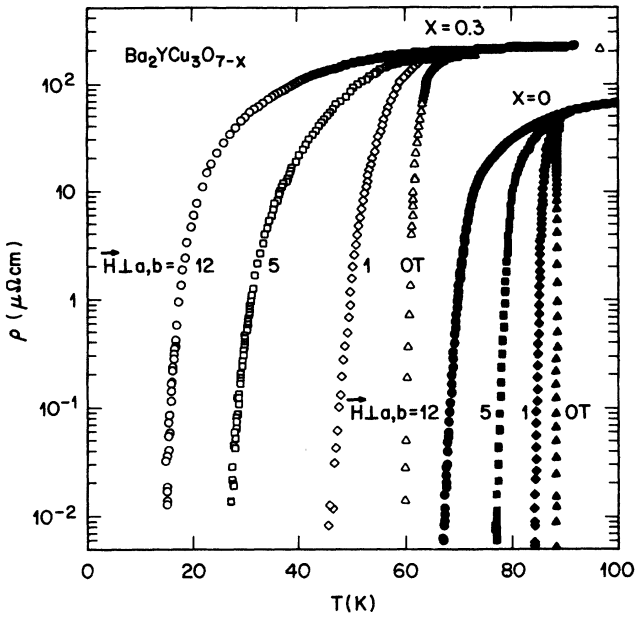

FIG. 13. Temperature dependence of the 60-K and 90-K phases of $Ba_2YCu_3O_{7-x}$ for $x=0$ and 0.3 on a semilogarithmic scale for several magnetic fields perpendicular to the Cu-O planes.

which will be discussed in a subsequent section; (2) a comparison of $Ba_2YCu_3O_7$ ($T_c \approx 90$ K) with $Ba_2YCu_3O_{6.7}$ ($T_c \approx 60$ K), which is given below.

In Fig. 13 we show the resistive transition of the 90- and 60-K phases of $Ba_2YCu_3O_{7-x}$. The resistive broadening for the 60-K phase in magnetic fields is almost as large as for the Bi compound, which means in our interpretation that the activation energies for flux motion are similar. This means that the activation energies for the 60-K phase are much smaller than for the 90-K phase, even though both the 90- and 60-K phases are orthorhombic and thus both have twin planes and a similar defect structure. Our explanation of this change in the activation energy is that the depletion of the oxygen chains, upon going from the 90- to the 60-K phase, decreases the electronic coupling between the $[CuO_2]$ double layers. Consequently, the 60-K phase is far more anisotropic than the 90-K phase. The resulting larger anisotropy reduces the correlation length L_c along the flux line and hence the activation energies.

It would be interesting to measure the thickness dependence of U_0. For the Bi compound we found similar activation energies for a 250 Å film, as for the 1-μm thick crystal. This suggests that L_c is smaller than 250 Å for this material. We expect 90-K phase $Ba_2YCu_3O_7$ to be much more in the two-dimensional pinning regime (straight flux lines).

In Fig. 14 we show a comparison of the flux creep behavior of various compounds, including $Tl_2Ba_2CaCu_2O_8$ and $Pb_2Sr_2RCaCu_3O_8$, for a magnetic field of 5 T perpendicular to the basal planes. The transitions are normalized for the transition temperature T_c and the normal-state resistivity ρ_n. We associate the broadening of the resistive transition with the electronic anisotropy, or equivalently with the tilt modulus of the flux lines for the various materials. Apparently, the Tl compound is even more anisotropic than the Bi compound. From this plot it is clear that the 90-K-phase $Ba_2YCu_3O_7$ is by far the least anisotropic and therefore this material has the largest activation energies for flux motion. Furthermore, we expect that the anisotropy of compounds in homologous series, i.e., with equivalent building blocks between the $[CuO_2]_\infty$ layers, is similar. This means that the activation energies for flux motion for the various Bi and Tl compounds are of the same magnitude, but much smaller than $Ba_2YCu_3O_7$. In conclusion, anisotropic materials will always have lower activation energies than isotropic superconductors, such as the $A15$ compounds, even if they have a similar defect structure.

F. Model for $Ba_2YCu_3O_7$

The resistive transition of single crystal $Ba_2YCu_3O_7$ was recently discussed by Tinkham in terms of flux creep.[5] He proposed that the resistance due to flux creep has the same dependence on the energy barrier as in the case of dissipation due to thermally activated phase motion in a heavily damped current-driven Josephson junction. The latter case was worked out theoretically and gives

$$\rho/\rho_n = [I_0(U_0/2)]^{-2} , \tag{11}$$

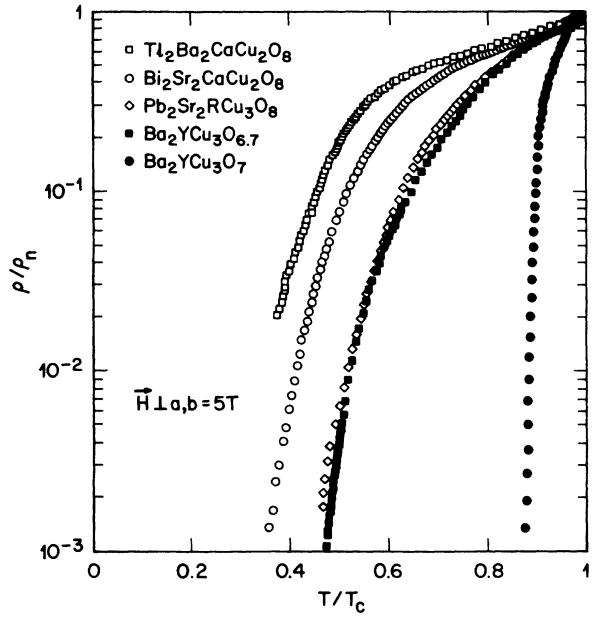

FIG. 14. Temperature dependence of the electrical resistivity of several high-temperature superconductors: $Tl_2Ba_2CaCu_2O_8$, $Bi_2Sr_2CaCu_2O_8$, $Pb_2Sr_2RCu_3O_8$, $Ba_2YCu_3O_{6.7}$, and $Ba_2YCu_3O_7$. The data are normalized for the transition temperature and the normal-state resistivity, and were taken in a field of 5 T perpendicular to the Cu-O planes. The difference in dissipation is related to the elastic constants of the flux line lattice (see text).

with I_0 the modified Bessel function. The activation energy was taken from Ref. 2, in which the activation energy is taken of the order of the condensation energy for a fluxon of length ξ_c:

$$U_0 \approx (H_c^2/8\pi) a_0^2 \xi_c \ . \tag{12}$$

This results in a temperature and magnetic field dependence of U_0:

$$U_0 \propto (1-t)^{3/2}/B \ . \tag{13}$$

This combination was used to describe the "visible resistive width" of the transition, which results in an impressive fit to the experimental data.

It is interesting to compare this formula with the data extending to five decades below the normal state. It should be noted that Tinkham fits the "visible resistive width" of resistivity ($\rho > 1\% \rho_n$), whereas the Arrhenius behavior of the resistivity only holds for low resistivities ($\rho < 1\% \rho_n$). Using the "best-fit" parameters on a linear resistivity scale, we reproduce Tinkham's results in the upper panel of Fig. 15 (open symbols). Using the same activation energies we replot these data on a logarithmic resistivity scale in the lower panel of Fig. 15. It is evident that the activation energies from the upper panel are much lower than the values inferred from the experimental data at low resistivities. We note that this model has only one adjustable parameter, and represents the experimental data only over a limited range. Furthermore, we were unable to obtain a reasonable fit of Eq. (11) using $U_0 \propto (1-t)^p/B^q$ for any value of p and q.

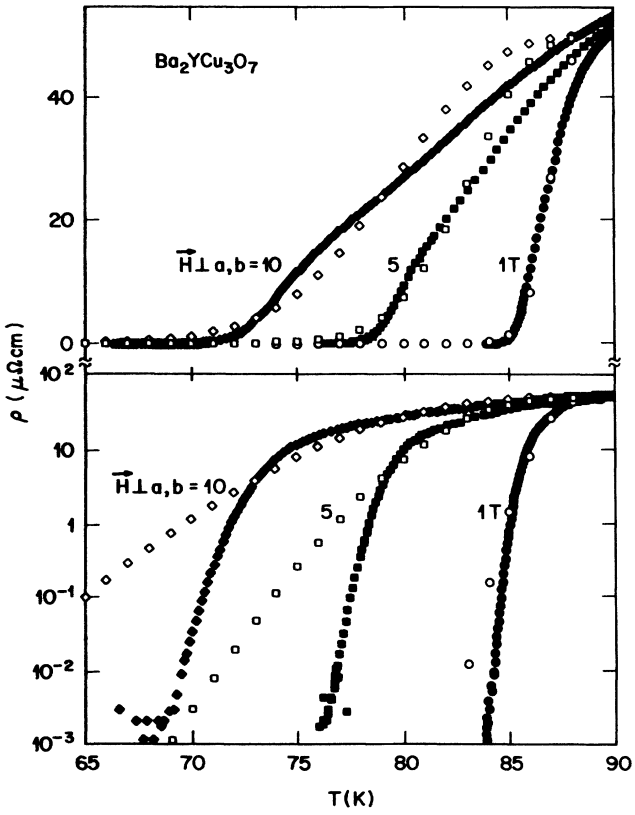

FIG. 15. Fit of the theoretical formula [Eq. (11), open symbols] to the experimental data (solid symbols). The upper panel shows the resistivity on a linear scale, and the lower panel on an exponential scale. Note that the theory has only one adjustable parameter.

Obviously, the temperature and magnetic field dependence of the pinning energy is different than predicted from this scaling argument. We think that the vanishing of the pinning energies at T_x, as shown in Fig. 9, reflects the temperature at which the pinning energies become comparable to $k_B T$ (e.g., $T_x \simeq 75.5$ K for $H_\perp = 10$ T). Therefore, any flux creep model is only applicable in the temperature regime below T_x. This temperature T_x delineates the thermally activated regime from the diffusive regime.[19,26] This temperature T_x is not necessarily the thermodynamic transition temperature. As this temperature regime around T_x is dominated by various dissipative processes such as flux creep, flux flow, superconducting fluctuations, and vortex-antivortex depairing, a correct description of this regime is difficult but certainly warranted.

G. Dynamic Experiments

In this section we want to relate our dc-resistivity measurements with ac measurements, viz., time dependence of the remanent magnetization, ac susceptibility, and mechanical oscillator experiments. Large flux creep effects were inferred from a large time dependence of the remanent magnetization.[2] The measurements inferred values of the activation energy $U_0 \approx 100$ K for $Ba_2YCu_3O_7$. This is significantly smaller than obtained from resistivity measurements. This difference originates from the intrinsic nature of a magnetization experiment. When a magnetic field is turned on below T_c shielding currents are generated. This brings the superconductor in the critical state, which means that ∇B is as large as pinning allows. In other words the shielding currents are of the order of the critical current. Consequently, this measurement technique probes a state far from the linear response regime, which is near $J \approx 0$. The critical state model is then used to extrapolate back to $J = 0$, assuming a linear dependence of U with J. This probably underestimates the zero-current activation energy U_0, as was already noted in early work on low-T_c materials,[30] but also in recent work on $Ba_2YCu_3O_7$ in which a logarithmic current dependence of the activation energy was found.[31] A more detailed analysis of this problem will be published separately.

Although magnetization is less suited to measure the activation energy, it can be used to measure the value of the critical current.[32] The critical current can be deduced from the width in the magnetization curve ΔM via a relation due to Bean.[33] This works as long as the sweep rate of the magnetic field is larger than the creep rate of the magnetization. Especially at large temperature where creep becomes dominant the Bean model is inappropriate to describe the experimental results. Therefore, the large field dependence of the critical current in $Bi_2Sr_2CaCu_2O_8$ deduced from $M(H)$ loops reflects mainly the large creep

effects, and not necessarily a pinning energy which changes rapidly with temperature.

Still, it is possible to measure the activation energy U_0 magnetically, e.g., with ac susceptibility.[10,11] The ac field, superimposed on a (larger) dc field, should have such small amplitude that the generated shielding currents are much smaller than the critical current. In this case the ac-susceptibility transition measures the response of the superconductor. Assuming a fairly narrow distribution of pinning energies,[24] we suggest that the response is given by a simple Debye relaxation:

$$\chi(\omega)=\frac{\chi(0)}{1+i\omega\tau} . \tag{14}$$

A transition in χ', accompanied by a peak in the dissipation χ'', occurs if the measuring frequency ω_m couples resonantly into the dynamics of the vortex system:

$$\omega_m\tau=1 , \tag{15}$$

with τ the relaxation time of the vortex system. Assuming that the dynamics is thermally activated the effective hopping rate $\nu_{\text{eff}}=\tau^{-1}$ is given by

$$\nu_{\text{eff}}=\nu_0\exp(-U_0/k_BT) , \tag{16}$$

with ν_0 an attempt frequency. Combining these equations we find that the maximum dissipation occurs at a temperature

$$T_{\text{dis}}=\frac{1}{\ln(\nu_0/\nu_m)}U_0(H)/k_B . \tag{17}$$

The peak in the dissipation signal χ'' does not indicate T_c but the temperature at which the measuring frequency and the relaxation time of the vortex system are the same.

From the dc-resistivity data we obtained the value for $U_0(H)$ and an estimate for the attempt frequency $\nu_0\approx 10^{12}$ Hz, neglecting the temperature dependence of $U_0(t)$ because we consider mostly small reduced temperatures $t<0.5$. Thus, T_{dis} can be calculated for any given magnetic field and measurement frequency without adjustable parameters. In Fig. 16 T_{dis} is shown for measurement frequencies of 1, 2×10^3, 10^6, and 10^9 Hz. Good agreement is found with ac-susceptibility measurements. This suggests that thermally activated dynamics describes the dc resistivity and ac susceptibility equally well. Alternatively, the ac-susceptibility measurements can be used to obtain $U_0(H)$ and ν_0, using a thermally activated model.

The analog between the dc resistivity and ac susceptibility can be seen even clearer by rewriting Eq. (17) as

$$\nu_m/\nu_0=\exp(-U_0/k_BT) , \tag{18}$$

in comparison to the experimentally observed resistivity which scales as

$$\rho/\rho_0=\exp(-U_0/k_BT) . \tag{19}$$

This close analogy shows that taking a resistance criterion is equivalent with taking a fixed frequency for an ac-susceptibility measurement (see Fig. 17). Therefore, a resistivity criterion cannot be used to measure the upper

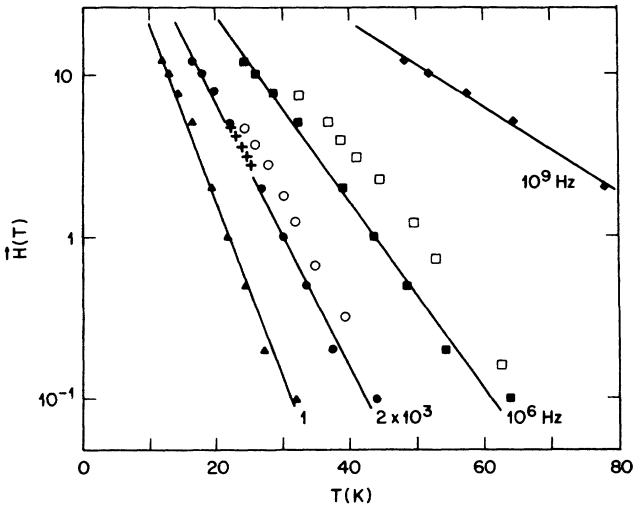

FIG. 16. Thermally activated dynamics as inferred from resistivity measurements: $\nu(H,T)=\nu_0\exp(-U_0/k_BT)$, results in dissipation peaks when $\nu(H,T)=\nu_{\text{meas}}$. Solid symbols: Calculated $\omega\tau=1$ conditions for various frequencies, using parameters from resistivity measurements (U_0 taken from Fig. 4 and $\nu_0\simeq10^{12}$ Hz). There are no adjustable parameters. Open symbols: Measured dissipation maxima at the same frequencies: ○, ac susceptibility at 2 kHz from Gammel *et al.*; □, ac susceptibility at 1 MHz from Worthington *et al.*; +, mechanical oscillator at 2 kHz from Gammel *et al.*

critical field. For $\nu_0\approx10^{12}$ and $\rho_0\approx10^5$ $\mu\Omega$ cm a resistivity criterion of 0.1 $\mu\Omega$ cm corresponds to a frequency of 1 MHz or an ac-susceptibility measurement of 1 MHz.

Previously, the dissipation temperature T_{dis} was denoted as the irreversibility line.[3] Indeed, this temperature gives the transition from a responding ($T>T_{\text{dis}}$) to a nonresponding system ($T<T_{\text{dis}}$). However, this interpretation makes it clear that this temperature depends on the time scale of the measurement.[34]

It is interesting to mention that the temperature at which maximum dissipation occurs in mechanical oscillator experiments[12] coincides with the "$\omega\tau=1$" criterion (see Fig. 16). This dissipative peak has been associated with flux lattice melting, and it will be interesting to clarify whether these measurements also probe the thermally activated dynamics of the vortex system. It is not completely clear whether the dynamics depends on the dissipation level of the measurement (mechanical oscillator $P>10^{-20}$ W, ac susceptibility $P>10^{-15}$ W, and resistivity $P>10^{-10}$ W. Comparing flux creep with the escape rate of a particle over a potential barrier,[35] there are three parameters determining the relaxation time τ: (1) the curvature of the bottom of the potential well, (2) the curvature of the top of the potential well, and (3) the damping rate. The fact that τ seems to vary so little for different dissipation levels suggests that the damping rate is essentially independent of the dissipation level.

It should be noted that we cannot rule out a phase transition at yet lower temperatures.[36,25] Namely, for temperatures above a phase transition thermally activat-

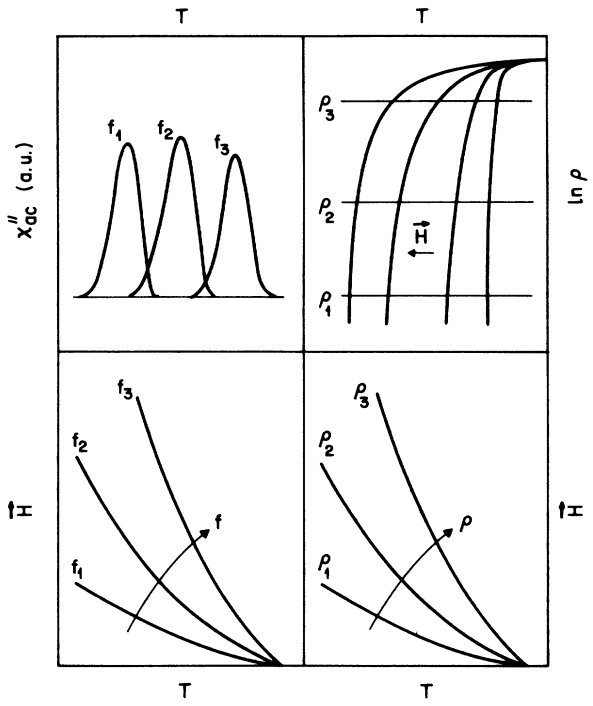

FIG. 17. Relation between ac susceptibility and dc resistivity criterion for a resistance measurement (schematically shown in upper right corner, cf. Fig. 8) corresponds to peak in the dissipation of an ac-susceptibility measurement at fixed frequency (upper left corner). Both procedures give an identical line in the H-T phase diagram, characterized by $\omega\tau=1$ (see text).

ed dynamics gives a good description, e.g., for spin-glass dynamics, etc. This transition could be observed when measuring at yet lower frequencies or smaller resistivities. As a final remark we note that high-frequency measurements (>1 GHz) are not influenced by flux creep effects except very near T_c, as can be seen from Fig. 16.

H. Low-temperature superconductors

Thermally activated resistivity behavior has been observed in various low-temperature superconductors, although it has never been interpreted as flux creep. We indicated that flux creep effects (or low activation energies) can be expected for compounds with large anisotropy or very thin films. Indeed, these materials have been reported to exhibit large resistive broadening, which we associated with flux creep.

A prominent example is thin film amorphous Mo-Ge, in which a thermally activated resistivity was observed over four decades in resistivity.[37] This behavior was discussed as "new universal resistive behavior of two-dimensional superconductors," but it is fully consistent with a flux creep model. The authors concluded from the Arrhenius law behavior that the activation energy is temperature independent, but overlooked for the possibility that $U_0(t)=U_0(0)(1-t)$ also gives Arrhenius law behavior, as shown above. Combining this temperature behavior with the observed[37] magnetic field dependence, these Mo-Ge thin films exhibit an activation energy which scales like $U_0(t)=U_0(0)(1-t)/B^{2/3}$. This differs from the relation suggested[2] for $Ba_2YCu_3O_7$: $U_0(t)=U_0(0)(1-t)^{3/2}/B$. The origin of this difference requires further study.

Further, the activation energy is proportional to the thickness of the amorphous Mo-Ge film. This means that the flux line correlation length L_c is larger than the sample thickness $d=100$ Å, indicating straight flux lines, or two-dimensional pinning.

The resistive transition of Mo-Ge thin films resembles the behavior of $Ba_2YCu_3O_7$ in the sense that the Arrhenius behavior sets in close to T_c. In contrast, the Bi compound resembles much more thin film In-In_2O_3, in which, also, thermally activated behavior was observed, however much below T_c.[38] For these two materials the resistance has a sharp initial decrease in resistance before entering the thermally activated regime. The data of In-In_2O_3 were interpreted as the activation energies $U_0(t)$ going to zero well below the thermodynamic transition temperature. Whether this is also true for the Bi compound has yet to be established.

A difficulty with Mo-Ge and In-In_2O_3 thin films is the restricted ohmic dissipation regime. This problem is much less in granular aluminum films, in which ohmic dissipation was observed over three decades in current density.[39] These data, interpreted as flux flow with anomalously small depinning critical currents, also fit a flux creep description. Replotting the original data gives activation energies of the order of 10 K for magnetic fields between 10^{-2} and 10^{-1} T.

A second class of materials in which large flux creep effects can be expected are the (intercalated) layered compounds, such as $NbSe_2$ and TaS_2,[29,40] and artificial multilayers.[41] However, the low defect density in the layered compounds makes it difficult to perform measurements in the ohmic dissipation regime. Obviously, the "conventional" criteria for T_c including zero resistivity or the maximum in the out-of-phase component of the ac susceptibility also fail for these compounds. Our preliminary measurements on $NbSe_2$ indicate that the resistive broadening can be described in a flux creep model, with activation energies between 100 and 1000 K for magnetic fields between 0.5 and 5 T. While flux creep effects are so clearly observed in high-temperature superconductors, they can also be studied in low-T_c compounds, and a more detailed comparison appears highly desirable.

IV. CONCLUSIONS

Resistance measurements of the superconducting transition of the high-temperature superconductors give insight into the flux pinning properties of the various materials. From these measurements we have extracted two parameters, the activation energy and the attempt frequency for flux creep. The activation energy appears to be the largest for $Ba_2YCu_3O_7$, and much smaller for the Bi and Tl compounds and $Pb_2Sr_2RCu_3O_8$. This difference in pinning can be related to the difference in anisotropy or the tilt modulos of the flux lines, determined to a large extent by the interplanar electronic coupling strength.

It is shown that ac experiments probe the dynamics of the flux lines. These measurements can be described using thermally activated dynamics. This model gives the intricate relationship between dc-resistivity and ac-susceptibility measurements, resulting in a peak in the dissipative signal if $\omega\tau=1$, with ω the probe frequency, and τ the relaxation time of the flux line lattice. It is argued that the irreversibility line and the melting transition also probe this $\omega\tau=1$ effect.

ACKNOWLEDGMENTS

We gratefully acknowledge stimulating discussions with D. J. Bishop, S. N. Coppersmith, R. C. Dynes, A. T. Fiory, D. S. Fisher, P. L. Gammel, E. M. Gyorgy, A. F. Hebard, D. A. Huse, M. Inui, P. B. Littlewood, A. P. Malozemoff, S. Martin, A. Millis, A. P. Ramirez, J. M. Valles, C. M. Varma, and T. K. Worthington.

[1]K. A. Muller, M. Takashige, and J. G. Bednorz, Phys. Rev. Lett. **58**, 1143 (1987).

[2]Y. Yeshurun and A. P. Malozemoff, Phys. Rev. Lett. **60**, 2202 (1988).

[3]A. P. Malozemoff, L. Krusin-Elbaum, D. C. Cronemyer, Y. Yeshurun, and F. Holtzberg, Phys. Rev. B **38**, 6490 (1988).

[4]T. T. M. Palstra, B. Batlogg, L. F. Schneemeyer, and J. V. Waszczak, Phys. Rev. Lett. **61**, 1662 (1988).

[5]M. Tinkham, Phys. Rev. Lett. **61**, 1658 (1988).

[6]T. T. M. Palstra, B. Batlogg, R. B. van Dover, L. F. Schneemeyer, and J. V. Waszczak, Appl. Phys. Lett. **54**, 763 (1989).

[7]J. D. Hettinger, A. G. Swanson, W. J. Skocpol, J. S. Brooks, J. M. Graybeal, P. M. Mankiewich, R. E. Howard, B. L. Straughn, and E. G. Burkhardt, Phys. Rev. Lett. **62**, 2044 (1989).

[8]J. Z. Sun, K. Char, M. R. Hahn, T. H. Geballe, and A. Kapitulnik, Appl. Phys. Lett. **54**, 663 (1989).

[9]Y. Iye, S. Nakamura, and T. Tamegai, Physica C **159**, 433 (1989).

[10]T. K. Worthington, Y. Yeshurun, A. P. Malozemoff, R. M. Yandrowski, F. H. Holtzberg, and T. R. Dinger, J. Phys. (Paris) **C8**, 2093 (1988).

[11]P. H. Kes, J. Aarts, J. van den Berg, C. J. van der Beek, J. A. Mydosh, Supercond. Sci. Technol. **1**, 242 (1989).

[12]P. L. Gammel, L. F. Schneemeyer, J. V. Waszczak, and D. J. Bishop, Phys. Rev. Lett. **61**, 1666 (1988).

[13]S. Gregory, C. T. Rogers, T. Venkatesan, X. D. Wu, A. Inam, and B. Dutta, Phys. Rev. Lett. **62**, 1548 (1989).

[14]P. L. Gammel, D. J. Bishop, G. J. Dolan, J. R. Kwo, C. A. Murray, L. F. Schneemeyer, and J. V. Waszczak, Phys. Rev. Lett. **59**, 2592 (1987).

[15]G. J. Dolan, F. Holtzberg, C. Feild, and T. R. Dinger, Phys. Rev. Lett. **62**, 2184 (1989).

[16]L. F. Schneemeyer, J. V. Waszczak, T. Siegrist, R. B. van Dover, L. W. Rupp, B. Batlogg, R. J. Cava, and D. W. Murphy, Nature **328**, 601 (1987).

[17]L. F. Schneemeyer, R. B. van Dover, S. H. Glarum, S. A. Sunshine, R. M. Fleming, B. Batlogg, T. Siegrist, J. H. Marshall, J. V. Waszczak, and L. W. Rupp, Nature **332**, 422 (1988).

[18]R. J. Cava, B. Batlogg, J. J. Krajewski, L. W. Rupp, L. F. Schneemeyer, T. Siegrist, R. B. van Dover, P. Marsh, W. F. Peck, P. K. Gallegher, S. H. Glarum, J. H. Marshal, R. C. Farrow, J. V. Waszczak, R. Hull, and P. Trevor, Nature **336**, 211 (1988).

[19]S. Martin, A. T. Fiory, R. M. Fleming, G. P. Espinoza, and A. S. Cooper, Phys. Rev. Lett. **62**, 677 (1989).

[20]P. A. Bancel and K. E. Gray, Phys. Rev. Lett. **46**, 148 (1981).

[21]P. W. Anderson, Phys. Rev. Lett. **9**, 309 (1962).

[22]Y. B. Kim, C. F. Hempstead, and A. R. Strnad, Phys. Rev. **131**, 2486 (1963).

[23]J. Bardeen and M. J. Stephen, Phys. Rev. A **140**, 1197 (1965).

[24]C. W. Hagen and R. Griessen, Phys. Rev. Lett. **62**, 2857 (1989).

[25]M. P. A. Fisher, Phys. Rev. Lett. **62**, 1415 (1989).

[26]A. F. Hebard, P. L. Gammel, C. E. Rice, and A. F. J. Levi, Phys. Rev. B **40**, 5243 (1989).

[27]S. Martin, A. T. Fiory, R. M. Fleming, L. F. Schneemeyer, and J. V. Waszczak, Phys. Rev. Lett. **60**, 2194 (1988).

[28]D. E. Farrel, S. Bonham, J. Foster, Y. C. Chang, P. Z. Jiang, K. G. Vandervoort, D. J. Lam, and V. G. Kogan, Phys. Rev. Lett. **63**, 782 (1989).

[29]Compare the resistive transitions of the high-T_c materials with the data on various intercalated (layered) materials. See, e.g., D. E. Prober, R. E. Scwall, and M. R. Beasley, Phys. Rev. B **21**, 2717 (1980); B. W. Pfalzgraf and H. Speckels, J. Phys. C **27**, 4359 (1987), and references therein.

[30]M. R. Beasley, R. Labusch, and W. W. Webb, Phys. Rev. **181**, 682 (1969).

[31]E. Zeldov, N. M. Amer, G. Koren, A. Gupta, R. J. Gambino, and M. W. McElfresh, Phys. Rev. Lett. **62**, 3093 (1989).

[32]See, e.g., E. M. Gyorgy, R. B. van Dover, S. Jin, R. C. Sherwood, L. F. Schneemeyer, T. H. Tiefel, and J. V. Waszczak, Appl. Phys. Lett. **53**, 2223 (1989).

[33]C. P. Bean, Phys. Rev. Lett. **8**, 250 (1962).

[34]A. P. Malozemoff, T. K. Worthington, Y. Yeshurun, F. Holtzberg, and P. K. Kes, Phys. Rev. B **38**, 7203 (1988).

[35]S. Chandrasekhar, Rev. Mod. Phys. **15**, 1 (1943).

[36]D. R. Nelson, Phys. Rev. Lett. **60**, 1973 (1988).

[37]J. M. Graybeal and M. R. Beasley, Phys. Rev. Lett. **56**, 173 (1986).

[38]J. C. Garland and Hu Jong Lee, Phys. Rev. B **36**, 3638 (1987).

[39]P. M. Horn and R. D. Parks, Phys. Rev. B **4**, 2178 (1971).

[40]J. A. Wilson and A. D. Yoffe, Adv. Phys. **18**, 193 (1969).

[41]The analysis of dimensional crossover in these systems probably should be reconsidered in the context of the present discussion. See, e.g., M. G. Karkut, V. Matijasvic, L. Antognazza, J.-M. Triscone, N. Missert, M. R. Beasley, and Ø. Fischer, Phys. Rev. Lett. **60**, 1751 (1988), and references therein.